Global Change Biology

Global Change Biology (2013), doi: 10.1111/gcb.12451

Climate change implications of shifting forest management strategy in a boreal forest ecosystem of Norway

RYAN M. BRIGHT*, CLARA ANTÓN-FERNÁNDEZ†, RASMUS ASTRUP†, FRANCESCO CHERUBINI*, MARIA KVALEVÅG‡ and ANDERS H. STRØMMAN*

Industrial Ecology Program, Energy and Process Engineering, Norwegian University of Science and Technology, Høgskoleringen 5, E-1, 7491 Trondheim, Norway, †Norwegian Forest and Landscape Institute, P.O. Box 115, 1431 Ås, Norway, ‡Center for International Climate and Environmental Research – Oslo (CICERO), P.O. Box 1129, Blindern, 0318 Oslo, Norway

Abstract

Empirical models alongside remotely sensed and station measured meteorological observations are employed to investigate both the local and global direct climate change impacts of alternative forest management strategies within a boreal ecosystem of eastern Norway. Stand-level analysis is firstly executed to attribute differences in daily, seasonal, and annual mean surface temperatures to differences in surface intrinsic biophysical properties across conifer, deciduous, and clear-cut sites. Relative to a conifer site, a slight local cooling of −0.13 °C at a deciduous site and −0.25 °C at a clear-cut site were observed over a 6-year period, which were mostly attributed to a higher albedo throughout the year. When monthly mean albedo trajectories over the entire managed forest landscape were taken into consideration, we found that strategies promoting natural regeneration of coniferous sites with native deciduous species led to substantial global direct climate cooling benefits relative to those maintaining current silviculture regimes – despite predicted long-term regional warming feedbacks and a reduced albedo in spring and autumn months. The magnitude and duration of the cooling benefit depended largely on whether management strategies jointly promoted an enhanced material supply over business-as-usual levels. Expressed in terms of an equivalent CO_2 emission pulse at the start of the simulation, the net climate response at the end of the 21st century spanned −8 to −159 Tg-CO_2-eq., depending on whether near-term harvest levels increased or followed current trends, respectively. This magnitude equates to approximately −20 to −300% of Norway's annual domestic (production) emission impact. Our analysis supports the assertion that a carbon-only focus in the design and implementation of forest management policy in boreal and other climatically similar regions can be counterproductive – and at best – suboptimal if boreal forests are to be used as a tool to mitigate global warming.

Keywords: albedo, boreal forest, global warming, net ecosystem exchange, RCP, remote sensing, surface temperature

Received 10 July 2013 and accepted 9 October 2013

Introduction

Boreal forests cover roughly 14.5% of the land surface and 27% of the forest area, making them the second largest forest biome (Gower *et al.*, 2001). The boreal forest is one of Norway's largest renewable resources, the majority of which is under active management. In addition to offering a variety of economic, environmental, and socio-cultural benefits, active forest management can contribute to climate protection through carbon sequestration (Canadell & Raupach, 2008; Ciais *et al.*, 2008; Pan *et al.*, 2011; Rautiainen *et al.*, 2011; Mackey *et al.*, 2013) and via the regulation of water and energy fluxes between the forest surface and atmosphere (Bonan, 2008; Jackson *et al.*, 2008; Anderson *et al.*, 2010).

Correspondence: Ryan M. Bright, tel. +47 735 98972; fax. +47 735 98943; email: ryan.m.bright@ntnu.no

Strategies to mitigate climate change involving forest management are often evaluated in terms of their carbon sequestration potential without considering biogeophysical implications (Hudiburg *et al.*, 2011; Holtsmark, 2012; Lamers *et al.*, 2013) – despite the overwhelming evidence from climate simulation (Bala *et al.*, 2007; Bathiany *et al.*, 2010; Davin & De Noblet-Ducoudré, 2010; Swann *et al.*, 2011) and observation-based studies (Lee *et al.*, 2011; West *et al.*, 2011; Houspanossian *et al.*, 2013) that such considerations can be of large importance, particularly at local and regional scales. Changes in forest cover can alter turbulent energy fluxes (sensible and latent heat) (Chapin *et al.*, 2000; Amiro *et al.*, 2006; Bond-Lamberty *et al.*, 2009) as well as the aerodynamic roughness of the land surface (Steyaert & Knox, 2008; Pongratz *et al.*, 2010; Pielke *et al.*, 2011) which can have local direct (Juang *et al.*, 2007; Lee *et al.*, 2011) and global indirect climate

consequences (Bathiany *et al.*, 2010; Davin & De Noblet-Ducoudré, 2010; Swann *et al.*, 2010, 2011). In many boreal regions, top-of-the-atmosphere (TOA) radiative imbalances from surface albedo perturbations can largely counteract those arising from concomitant changes to the terrestrial carbon-cycle and atmospheric CO_2 concentrations (Betts, 2000; Randerson *et al.*, 2006; Lohila *et al.*, 2010; Bright *et al.*, 2011; Pongratz *et al.*, 2011; Cherubini *et al.*, 2012; O'halloran *et al.*, 2012). Management strategies with climate protection goals therefore risk being counterproductive when key biogeophysical factors – notably surface albedo changes – are excluded from climate impact assessments in these regions (Betts, 2000, 2007; Marland *et al.*, 2003; Jackson *et al.*, 2008; West *et al.*, 2011; Anderson-Teixeira *et al.*, 2012; Mahmood *et al.*, 2013).

Management disturbance like clear-cut harvesting or species switching alters important biophysical properties which can have direct consequences on local climate. For instance, forests have been shown to dissipate sensible heat to the atmospheric boundary layer more efficiently relative to open landscapes, owed to their larger aerodynamic roughness (Rotenberg & Yakir, 2010; Lee *et al.*, 2011). Forests can also dispel latent heat more efficiently from the surface relative to open areas, depending on ambient moisture conditions and temperature (Baldocchi *et al.*, 2000; Eugster *et al.*, 2000; Von Randow *et al.*, 2004). Local surface temperatures are affected not only by albedo changes but also by energy redistribution through convection and evapotranspiration (Juang *et al.*, 2007; Lee *et al.*, 2011; Rocha & Shaver, 2011). Their relative contributions depend on environmental- (i.e. solar radiation, air temperature, water supply) as well as vegetation-dependent physical and structural attributes [i.e. stomatal conductance, rooting depth, leaf area index (LAI), canopy height, etc.]. The latter are modified and shaped directly by forest management, thus a deeper understanding of the relative importance of the various biophysical components likely to be affected is required in the design of climate-effective management policy.

Few studies have integrated biogeophysical components alongside carbon-cycle considerations when evaluating alternative management strategies directed at climate protection. Changes to forest management decision variables affecting harvest age (rotation period) or regeneration efforts (delayed planting) have been shown to optimize climate mitigation benefits when albedo change considerations are taken into account alongside carbon (Thompson *et al.*, 2009). In addition to changes in harvest or silviculture regimes, species conversion has also been proposed as an alternative strategy to leverage biophysical climate benefits of managed forests in some regions, particularly when deciduous species replace conifers (Anderson *et al.*, 2010). Summer and winter albedo of deciduous forests in boreal regions is generally higher than in conifer forests (Betts & Ball, 1997; Eugster *et al.*, 2000; Bright *et al.*, 2013; Lukeš *et al.*, 2013), and deciduous broadleaf species typically have higher canopy conductance to heat and water vapor transfer than conifers in summer (Baldocchi *et al.*, 2000; Eugster *et al.*, 2000; Blanken *et al.*, 2001; Wang & Dickinson, 2012). Across the boreal forest, the succession dynamics on upland sites after a natural or human-induced disturbance is rapid colonization of deciduous pioneer species (betula spp., populus spp.), which over time, is replaced by more shade-tolerant conifer species (picea and abies spp)(Chen & Popadiouk, 2002). Such rapid colonization by deciduous species can make dominant contributions to surface energy and carbon fluxes (Van Cleve *et al.*, 1996; Beck *et al.*, 2011). However, the prevailing industrial forest management regimes introduced post-1950 in both the Fennoscandic and Canadian boreal forest have promoted pure conifers (through planting and vegetation control) after harvest due to a higher economic value, and on average, higher wood production (Kuuluvainen, 2009). Despite current practice, the literature illustrates that management regimes that more closely resemble the natural dynamics where deciduous species are succeeded by conifers over time can be economically advantageous (Lieffers & Beck, 1994; Macdonald, 1995; Burton *et al.*, 2006) and beneficial for ecosystem services such as biodiversity (Christensen & Emborg, 1996; Fries *et al.*, 1997; Angelstam, 1998). Hence, in Norway (Granhus & Fløistad, 2010) and across the boreal belt in general, there is a significant interest in exploring management strategies that favor deciduous tree species.

Aims

By focusing on boreal Norway, we illustrate how regional forest management strategies might be better designed for climate protection when important biophysical considerations are included alongside carbon-cycle dynamics. We firstly execute a stand-level analysis whereby the relative importance of radiative, aerodynamic, and physiological properties to deviations in local surface temperature across deciduous, coniferous, and clear-cut sites are explored analytically using a combination of meteorological and remotely sensed observation. The analysis is meant to acquire an improved understanding of the fundamental drivers of surface temperature afforded by different forest types possessing stand attributes shaped by typical management practice throughout the case study region. Secondly, we carry out a regional simulation to investigate a business-as-usual (BAU) and three alternative forest

management scenarios for boreal Norway and their global direct climate consequences when empirically based predictive harvest and albedo models are employed in the analysis. The investigated alternative management strategies involve changes to harvest levels and regeneration regimes that include shifts toward a higher reliance on natural deciduous regeneration strategies. Thirdly, we investigate the magnitude of the future climate-albedo feedback under projected regional warming linked to representative concentration pathways (RCPs) 4.5 (Thomson *et al*., 2011) and 8.5 (Riahi *et al*., 2011).

The scope of our analysis is restricted to physical effects resulting from management-induced changes occurring within the forest; climate impacts linked to changes in the global supply and demand of wood products or to emissions connected to wood-product life cycles are excluded from the analysis as they require separate, detailed treatment.

Material and methods

Regional Geography and Climate

Inland regions of the south and east have historically been the most important forestry regions in Norway and are currently producing almost 75% of the domestic commercial timber supply. The forest in these regions may be considered part of the boreal forest that extends as an almost continuous belt around the upper northern hemisphere. Managed forests of the region (Fig. 1) are dominated by Norway spruce (*Picea abies* H. Karst.), Scots pine (*Pinus sylvestris* L.) and Birch (*Betula pendula* Roth and *B. pubescens* Ehrh.), with understory vegetation often dominated by bilberries (*Vaccinium myrtillus* L.), other Vaccinium species, and various herb communities (Granhus *et al*., 2012). Pine is dominant on dryer and poorer site types, while spruce is often found on more fertile sites. Birch is a pioneer deciduous species that is found throughout the forest, and continuous, low-productive birch forests dominate the high elevation areas of the region.

The region experiences a continental climate ('Subarctic/Boreal') characterized by long cold winters with short mild summers and moderate, seasonally distributed precipitation (Peel *et al*., 2007). Where logging activities are concentrated, snow covers the ground from December through early April in the lower elevations of the central, southern, and eastern parts of the region (ca. 200 m) – and from late October through early May in the northern and western parts of the region (ca. 800 m) (Norwegian Meteorological Institute, 2013).

Relative contributions to local surface temperature change

Using surface temperature as a metric for the stand-level analysis, the relative local direct climate change contributions resulting from perturbations in radiative, aerodynamic, and physiological properties in forests are explored analytically following the approach of Lee *et al*. (2011) with the following expression:

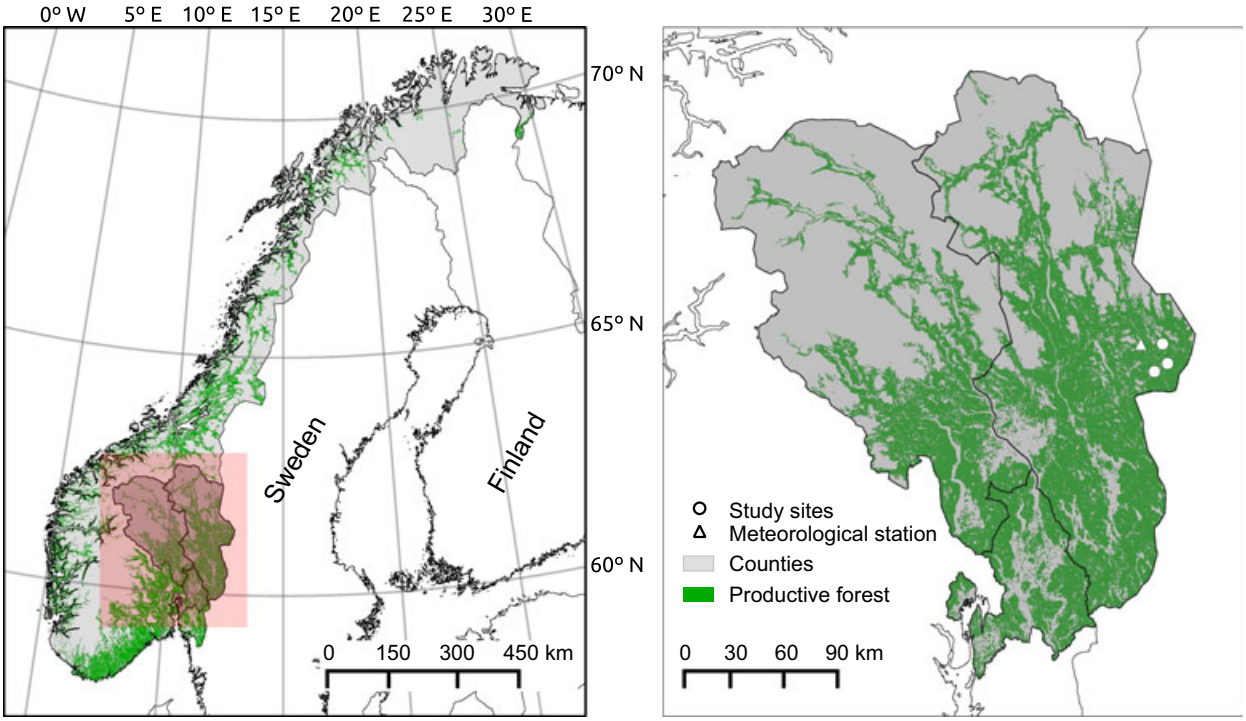

Fig. 1 2D spatial signature of the managed forest area included in the assessment which includes all areas labeled 'Productive forest' within the three highlighted counties shown (2.53 Mha in total). Sites included in our stand-level analysis are also indicated.

$$\Delta T_s \approx \frac{\lambda}{(1+f)}\Delta SW + \frac{-\lambda}{(1+f)^2}R_n\Delta f_1 + \frac{-\lambda}{(1+f)^2}R_n\Delta f_2 \quad (1)$$

where the first, second, and third terms on the right-hand side of Eqn. (1) give us the approximate contributions to a surface temperature change from an external albedo change forcing, an internal energy redistribution linked to aerodynamic roughness change, and an internal energy redistribution linked to Bowen ratio (i.e. the ratio of sensible to latent turbulent heat flux) changes, respectively. By identifying sites within close proximity to a regional meteorological station and to each other, we are able to combine meteorological and remote sensing datasets to attribute the relative contributions by the three main intrinsic biophysical mechanisms to the observed differences in surface temperature across a young clear-cut site (harvested 2003), an 80-year coniferous-dominant stand, and a 50-year deciduous-dominant stand over the period January 2004–December 2009. The sites are assumed to share the same background climate state, that is, they receive equal amounts of incoming short- and longwave radiation and share identical ambient climate parameters like air temperature, vapor pressure, relative humidity, etc. See Supporting Information for additional site and methodology details surrounding the stand-level analysis and our reformulation of the Lee *et al.* (2011) equation [Eqn. (1)].

MODIS 8-day Albedo/BRDF product MCD43B3 (Schaaf *et al.*, 2002) provides gridded estimates of black-sky shortwave broadband albedo at ca. 1 km^2 resolution and is used to compute changes in surface shortwave radiation (ΔSW) and net radiation (R_n). Net radiation R_n is the difference between incoming net shortwave radiation and outgoing net longwave radiation calculated following Allen *et al.* (1998) using daily insolation and clearness index data obtained from the NASA Langley Research Center POWER Project (NASA, 2013). The 8-day composites of MODIS diurnal mean surface temperature (MOD11A2) (Wan, 1999; Wan & Li, 2008) at ca. 1 km^2 resolution are used to estimate the climate sensitivity (λ) and energy redistribution expressions (f) of Eqn. (1).

Bowen ratios (β) are estimated with the sensible heat flux as the residual of the surface energy balance equation:

$$\beta = \frac{(R_n - LE - G)}{LE} \quad (2)$$

where LE is the latent heat flux from evaporation and transpiration estimated with an updated 8-day MODIS global evapotranspiration algorithm (MOD16A2, ca. 1 km^2 resolution) (Mu *et al.*, 2011) and G is the ground heat flux estimated using the Fraction of Absorbed Photosynthetically Active Radiation (FPAR) (MOD15A2, ca. 1 km^2 resolution) (Knyazikhin *et al.*, 1999) as a surrogate for fractional vegetation coverage (Los *et al.*, 2000) together with a soil heat flux ratio for a fully vegetated canopy of 0.05 (Monteith & Unsworth, 2008) and a soil heat flux ratio for bare soil of 0.315 (Kustas & Daughtry, 1990).

Aerodynamic resistance (r_a) to heat and momentum transfer is estimated for neutral conditions (stability parameters for heat and momentum equal zero) following refs. (Allen *et al.*, 1998; Liu *et al.*, 2007):

$$r_a = \frac{1}{k^2 u}\left[\ln\left(\frac{z-d}{z_m}\right)\right]\ln\left[\left(\frac{z-d}{z_h}\right)\right] \quad (3)$$

where z is a reference height of 10 m, k is the von Karman constant (0.41), u the wind speed at reference height (ms^{-1}), d the zero-plane displacement height (m), or the height at which wind speed becomes essentially zero in the canopy, z_m the roughness length for momentum transfer, and z_h the roughness length for heat transfer. Roughness lengths for momentum z_m and zero-plane displacement heights d are calculated using empirical models developed by Nakai *et al.* (2008) that are based on stand density SD (trees ha^{-1}), LAI (m^2 m^{-2}), and mean tree height h(m):

$$d = \left(1 - \left[\frac{1-\exp(-k_1 SD)}{k_1 SD}\right]\left[\frac{1-\exp(-k_2 LAI)}{k_2 LAI}\right]\right)h \quad (4)$$

where k_1 and k_2 are parameters and LAI is leaf area index, also taken from MOD15A2 (ca. 1 km^2 resolution) (Knyazikhin *et al.*, 1999). For the deciduous site, a stand density of ca. 1400 trees ha^{-1} and average tree height of 9 m are applied; for the coniferous site, a stand density of ca. 750 trees ha^{-1} and average tree height of 15 m are applied; the clear-cut site has a stand density of ca. 10 trees ha^{-1} (due to tree retention policy) with a mean tree height from 2004–2010 of 2 m. Roughness length for momentum is then estimated with the zero-plane displacement height, tree height, and an empirical constant:

$$z_m = 0.264(1 - \frac{d}{h})h \quad (5)$$

Following Allen *et al.* (1998), we assume the roughness length for heat, z_h, is 1/10th of z_m.

The remote sensing products (MODIS) are employed in their native spatial and temporal resolutions and filtered for quality, with single pixels centered over each stand. Missing data are imputed using means of available data for the same composite date from other years in the 6-year time series In the rare case when no high quality data for the full 6-year time series exist for a given composite date, values are linearly interpreted between the previous and succeeding high quality values. The gap-filled 8-day MODIS composites are applied together with the daily meteorological data for each of the 8 days comprising the production period. Uncertainties surrounding the remote sensing products employed are discussed in Supporting Information.

Scenario and modeling framework descriptions

A 21st-century simulation of harvest rates, albedo, and terrestrial C-cycle dynamics over 2.53 million hectares of productive (managed) forest is performed for a Business-as-Usual (BAU) reference and three alternative scenarios, described in Table 1. The BAU scenario is designed to illustrate the current timber extraction practice combined with the current forest regeneration practice whereby newly harvested coniferous sites are regenerated with the same coniferous species (*Picea abies* and *Pinus sylvestris*). The first alternative scenario (Fig. S1) illustrates a management regime where harvested stands are allowed to naturally regenerate with native deciduous species

Table 1 Forest management scenario descriptions

Scenario Acronym	Description
BAU	21st century business-as-usual (BAU) harvest rates with coniferous forests artificially regenerated with the same species as was harvested
S1	Same as BAU except that all harvested spruce- and pine-dominant stands with site indices ≥14* are allowed to naturally regenerate with birch
S2	Same as BAU but with the probability of final felling increased by 30%.
S3	Combination of S1 and S2: Increased harvest probability by 30% plus natural birch succession

*Site index is based on the H_{40} system, where 14 represents the mean tree height in meters at 40 years breast height age. An H_{40} of 14 m is the regional average.

(*Betula pen.* and *Betula pub*) rather than be artificially regenerated with conifers. The second alternative scenario (Fig. S2) is intended to illustrate an increased harvest activity which is in line with the political white papers in Norway (Norwegian Ministry of Food & Agriculture, 2009). The final alternative scenario (Fig. S3) is seen as a combination of Fig. S1 and S2 with both an increased harvest level and a practice that promotes natural site regeneration with deciduous species.

Simulations rely on data from the Norwegian National Forest Inventory (NFI) (Tomter *et al*., 2010) and a series of empirically based models for predicting regional harvest rates (Antón-Fernández & Astrup, 2012), carbon in live biomass (Antón-Fernández & Astrup, 2012), carbon in dead organic matter and soil (Liski *et al*., 2005), and surface albedo (Bright *et al*., 2013).

Final harvests and thinnings are estimated with an empirical harvest model (Antón-Fernández & Astrup, 2012) that predicts the probability of harvest for each plot based on forest attributes obtained from NFI data such as site productivity, stand age, volume, slope, and proximity to road. The advantage of this type of model is that it produces a realistic estimate of living biomass increments combined with a realistic forecast of harvest and thinning activity across the landscape with few assumptions.

The respiration model Yasso (Liski *et al*., 2005) is applied to simulate changes in carbon stocks in dead organic matter and soil pools. The advantage of the Yasso model is that it was designed to simulate C-dynamics in conjunction with data from standard forest inventory plots. We use a version that has been parameterized specifically for our case region as described in De Wit *et al*. (2006).

Regression models developed with chronosequences of remotely sensed albedo observations throughout the region are employed to estimate changes in surface albedo at monthly time increments (Bright *et al*., 2013). The models require inputs of average stand age, dominant tree species, and monthly mean air temperature and are capable of predicting monthly mean direct-hemispherical shortwave albedo with relatively high accuracy, with normalized root mean square errors (RMSE) ranging from 7 to 8%, depending on the dominant tree species.

In the BAU scenario, the predictive harvest model (Antón-Fernández & Astrup, 2012) determines the harvest and thinning levels and all harvested stands (final fellings) are regenerated with the same species as was harvested; in Fig. S1, harvested coniferous stands with medium site productivities are regenerated with deciduous species. For the two alternate scenarios with increased initial harvest levels (Figs. S2 and S3), plot-wise harvest probabilities predicted by the harvest model are multiplied by 1.3. Multiplying the probability of harvest by a factor (1.3) implies that the harvest will increase in the simulation but that the patterns of harvest across the landscape are maintained. This is analogous to a simulation where harvest increases are driven by increases in subsidies or timber prices.

Because the harvest model is a probabilistic model, all scenario outcomes are results of a Monte Carlo simulation executed with 1000 runs. The Monte Carlo approach – combined with the fact that all models employed are empirically based and have readily available estimates of uncertainty related to model parameters – provides the ability to estimate model error in the simulation. However, for simplicity, the model errors are generally not illustrated in the presented results (see Supporting Information).

Net Ecosystem Exchange

We apply the definition of Hayes *et al*. (2012) in calculations of Net Ecosystem Exchange (NEE) based on forest inventory estimates of stock changes adjusted for the lateral transfer of harvest removals:

$$\mathrm{NEE} = \Delta\mathrm{Live} + \Delta\mathrm{DOM} + \mathrm{HP} \quad (6)$$

where species-specific allometric equations (Marklund, 1988) are used to estimate changes in C stocks in living biomass (ΔLive), and changes in dead organic matter stocks (ΔDOM) are derived with the assistance of the soil carbon model (Liski *et al*., 2005) parameterized for regional climate conditions (i.e. temperature, soil moisture)(De Wit *et al*., 2006). Due to intensive forest management in Scandinavia, disturbances from forest fires have been mostly eliminated (Stocks *et al*., 1998) and were not simulated, thus only C in biomass removed from thinnings and final felling disturbances – or in the harvested product (*HP*) flux – is considered in estimates of NEE. In keeping with the conventional definition of NEE, negative values denote a net sequestration flux by the terrestrial C-sink while positive values denote a net emission flux to the atmosphere.

Global temperature change: Contributions from ΔNEE and Δalbedo radiative forcings

The difference in the NEE C-flux (CO_2 only) between an alternative management scenario and the BAU scenario represents the net biological carbon sequestered by the terrestrial biosphere or oxidized to the atmosphere. Resulting CO_2 concentration changes are estimated using the multimodel mean impulse response function (IRF) reported in Joos *et al.* (2013) that describes the atmospheric decay of CO_2 following a pulse emission to the atmosphere.

Radiative forcing for CO_2 is approximated following the expression from Myhre *et al.* (1998) based on radiative transfer models:

$$\mathrm{RF}_{\mathrm{CO_2}} = 5.35 \ln\left(\frac{\mathrm{CO_2} + \Delta\mathrm{CO_2}}{\mathrm{CO_2}}\right) \quad (7)$$

where CO_2 is the unperturbed, or the 2010 reference atmospheric CO_2 concentration of 389 ppmv (Conway & Tans, 2012), and ΔCO_2 is the change from the reference. An increase in radiative forcing due to a unit (kg) increase in the atmospheric abundance of CO_2 – or its radiative efficiency, k_{CO_2}, is expressed:

$$k_{\mathrm{CO_2}} = \frac{\Delta \mathrm{RF}}{\Delta \mathrm{CO_2}} \quad (8)$$

The radiative efficiency (see Figure S4 for values) is applied to compute instantaneous radiative forcings due to annual changes in the NEE C-flux:

$$\mathrm{RF}_{\Delta\mathrm{NEE}}(t) = k_{\mathrm{CO_2}} \int_0^t [\mathrm{NEE_S}(t') - \mathrm{NEE_{BAU}}(t')] y(t - t') \mathrm{d}t' \quad (9)$$

where y is the CO_2 IRF at the background concentration of 389 ppmv (Joos *et al.*, 2013) and NEE_S - NEE_{BAU} the NEE C-flux difference between any alternative and the BAU scenario after multiplication with the molecular weight ratio 44/12 to convert to CO_2 (in kg). Positive differences in NEE denote a concentration increase, while negative differences denote a decrease.

Global annual mean instantaneous shortwave radiative forcings at the top of Earth's atmosphere (TOA) from a monthly mean surface albedo change are calculated at one degree spatial resolution using a simple 1-layer transfer scheme (Cherubini *et al.*, 2012; Bright & Kvalevåg, 2013):

$$\mathrm{RF}_{\Delta\alpha}(t, i) = \frac{\sum_{m=1}^{m=12} -R_s(m, i) \Delta\alpha_s(m, t, i)}{12} T_a \left(\frac{A_{\mathrm{local}}(i)}{A_{\mathrm{global}}}\right) \quad (10)$$

where $\Delta\alpha_s$ is the mean surface albedo change in month m and year t in region i, R_s the 22-year mean down-welling solar radiation flux at surface level in month m for region i obtained from the NASA Langley Research Center POWER Project (NASA, 2013), T_a an up-welling atmospheric transmittance factor, A_{local} the local productive forest area in region i, and A_{global} the area of Earth's surface. T_a is a constant based on the globally averaged annual mean fraction of up-welling radiation exiting a clear-sky, or 0.85 (Lenton & Vaughan, 2009). The model [Eqn. (10)] has been tested and benchmarked to a more sophisticated radiative transfer model based on a discrete ordinate method (Bright & Kvalevåg, 2013).

A temperature IRF (Boucher & Reddy, 2008) is applied to convert a global instantaneous forcing into a global surface temperature change after adjusting model parameters to consider the differences in climate efficacy (Joshi *et al.*, 2003; Hansen *et al.*, 2005) between albedo change radiative forcings and radiative forcings from CO_2 concentration changes. We apply a conservative efficacy of 1.94 for a snow-albedo change (Cherubini *et al.*, 2012) which, in our case region, is the main driver of surface albedo change in forests (Bright *et al.*, 2013). This entails harmonizing climate sensitivity and response timescale parameters to account for model differences between that used to estimate the snow-albedo change efficacy parameter (HadGEM2) (Bellouin & Boucher, 2010) and the temperature IRF parameters (HadCM3), as described in refs. (Cherubini *et al.*, 2012, 2013):

$$\Delta T_s(t) = \int_0^t [\mathrm{RF}_{\Delta\mathrm{NEE}}(t') + \mathrm{RF}_{\Delta\alpha}(t')] \delta T(t - t') \mathrm{d}t' \quad (11)$$

where δT is the temperature IRF of Boucher & Reddy (2008), $RF_{\Delta NEE}$ the radiative forcing linked to NEE changes [Eqn. (9)], and $RF_{\Delta\alpha}$ the radiative forcing linked to albedo changes [Eqn. (10)].

Climate Change Feedback

Temperature seasonality – or the difference between winter and summer temperatures (Mann & Park, 1996) – has been diminishing over time in northern regions (Dye & Tucker, 2003; Xu *et al.*, 2013) and will continue to decrease under climate change. We investigate the resulting impacts on albedo using the multimodel (67) ensemble mean monthly local near surface temperature outcomes from representative concentration pathways (RCPs) 4.5 (Thomson *et al.*, 2011) and 8.5 (Riahi *et al.*, 2011) from the CMIP5 21st century experiments (KNMI, 2013), which are directly linked to our albedo model that utilizes air temperature as a predictor variable. Although changes in regional precipitation under climate change may also affect albedo in winter and spring via changes in snow frequency and ablation, it is excluded from our assessment due to modeling limitations.

The terrestrial C-balance in boreal ecosystems under a changing climate will be regulated ultimately by the difference between carbon gains via greater primary productivity and losses through organic matter decomposition. In our investigation of climate feedbacks, we focus on albedo and exclude the terrestrial C-cycle response. There is large inherent uncertainty in the response by soil decomposers to temperature (Lindroth *et al.*, 1998; Davidson & Janssens, 2006; Sistla *et al.*, 2013) as well as the vegetation response to changes in the surface water balance in the region (Lapenis *et al.*, 2005). Regional climate modeling has indicated that in neighboring Sweden, for example, reduced soil moisture levels can counterbalance the effect of a longer growing season and CO_2 fertilization on NPP, while temperature-driven increases in decomposition rates of soil organic matter can increase ecosystem respiration – with the potential for forests becoming a net C-source by the late 21st century under four regional climate change scenarios (Koca *et al.*, 2006). Recent modeling studies attempting to

analyze the overall global impact of projected future climate change on terrestrial ecosystem carbon storage generally reveal large differences across models in terms of the size and even the sign of the net change in NEE for our region (Friedlingstein *et al*., 2006; Sitch *et al*., 2008; Ahlström *et al*., 2012), indicating that a treatment of the C-cycle response deserves a separate, detailed treatment.

Results

Stand-level Local Temperature Impact Contributions

Mean results from the 6-year time series are presented in Fig. 2 The full time series is reported in Supporting Information (Fig. S5) together with the underlying remote sensing dataset (Fig. S1). Seasonal surface temperature differences (ΔT_s) driven by albedo differences between the clear-cut and two mature forested sites (Fig. 2a and b) and between the deciduous and coniferous site (Fig. 2c) show distinct patterns: the higher albedo of the clear-cut site relative to the two forested sites – and at the deciduous site relative to the coniferous site – dominates the relative ΔT_s (green), particularly in late winter and early spring when snow is still present and incoming solar radiation strengthens. Due to its lower LAI in winter, masking of snow by the forest canopy is less pronounced at the deciduous site, thus ΔT_s is less extreme (Fig. 2b, green) in winter compared to the coniferous case (Fig. 2a, green). Interestingly, ΔT_s in early spring between the two forested stands (Fig. 2c) is found to be greater than ΔT_s between the clear-cut and the deciduous stand (Fig. 2b).

As snow melts the relative importance of albedo diminishes and surface roughness and Bowen ratio differences begin to play a greater role. Relative warming at the clear-cut site due to a lower aerodynamic roughness results in higher aerodynamic resistance (Fig. S2) and less efficient convective heat transfer in summer months (Fig. 2a and b, magenta). While this effect dominates the net ΔT_s in summer relative to the deciduous stand (Fig. 2b), relative to the coniferous stand the effect is approximately offset by a higher snow-free albedo (Fig. 2A, green).

Similar warming trends at the clear-cut site in summer months can be observed due to a lower canopy conductance (lower transpiration) which results in a reduced partitioning of R_n into latent turbulent heat [relative Bowen ratio warming (Fig. 2a, b; cyan)] – although this effect is less prominent than the contribution from differences in roughness lengths (Fig. S2).

Relative to the coniferous site, the deciduous site experiences similar seasonal trends in albedo cooling and roughness warming as the clear-cut site (Fig. 2c, green and magenta); however, a larger portion of R_n is partitioned into latent heat during spring and summer months at the deciduous site, resulting in lower Bowen ratios and relative cooling (Fig. 2c, cyan). Together with its higher albedo during all seasons, lower spring and summer Bowen ratios at the deciduous site results in a combined cooling effect that offsets roughness warming leading to a net cooling (Fig. 2c, black) throughout most of the year relative to the coniferous site.

Global Direct Impacts from Regional ΔNEE and Surface Albedo Change

Means of the Monte Carlo simulation outcomes for each management scenario are presented in Fig. 3. Compared to the current NEE of -6.7 Tg C yr^{-1}, the additional harvesting at the start of the simulation (2014) in S2 (red) and S3 (green) results in an immediate increase (productivity loss) in NEE of around 1.2 Tg C yr^{-1}. In S1 (blue), the effect of allowing deciduous regeneration after coniferous harvests without increasing harvest levels enhances the overall C-sink capacity (i.e. productivity gain) of the forest during the first 30–40 years (Fig. 3, left, blue) due to a higher NPP flux at all harvested coniferous sites regenerated with birch during this time period. Regenerating harvested coniferous stands with deciduous species as in S1 and S3, however, results in a weakened total forest C-sink in the longer term. For example, NEE at 2100 in S1 and S3 is -2.6 and -2.7 Tg C yr^{-1}, respectively, while in BAU and S2, NEE is around -3.7 Tg C yr^{-1}, respectively. The general trend of a declining 21st century forest C-sink (increasing NEE) present in all scenarios reflects the forest age class and species composition resulting from historical management decisions of the 1940s–1960s to drastically increase planting of spruce and increase stocking densities, which ultimately led to the high productivity levels observed today.

The decline in harvested products in S1 and S3 toward the end of the century is due to the higher proportion of deciduous forest which translates into a lower predicted harvest probability by the harvest model (and thus less HP). Low harvest predictions by the model is a reflection of the current management practice in which deciduous harvests are rare due to the lower market value of birch and a regional forest industry structured around coniferous species.

When averaged over the year, total forest albedo (Fig. 3, right) significantly increases for both deciduous scenarios S1 and S3 compared to strategies involving the more traditional silviculture methods (regeneration with conifers), such as in scenario BAU and S2. This is due to reduced snow masking in winter and higher canopy albedo in summer as the share of total deciduous stand area increases. Albedo is increased some in

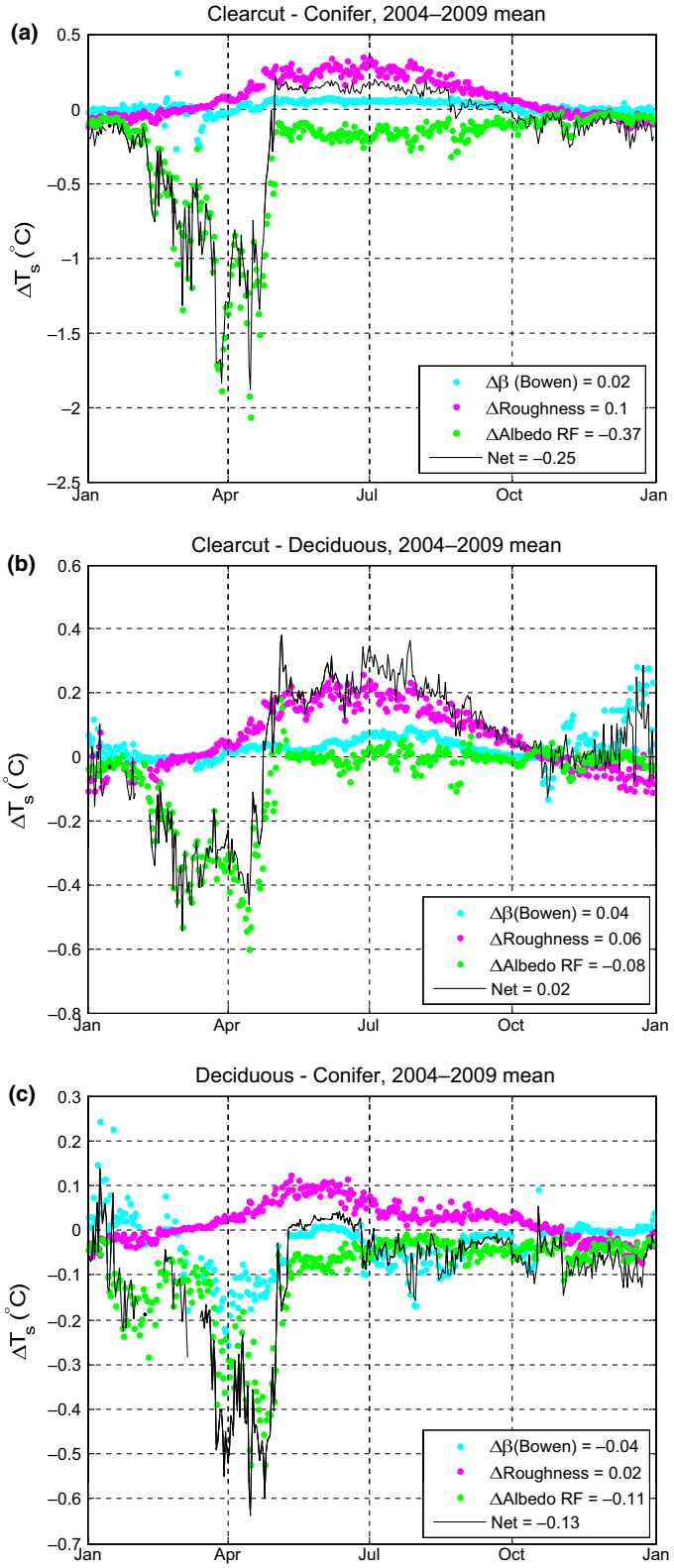

Fig. 2 Contributions to differences in local surface temperature across three managed sites due to differences in surface albedo ('ΔAlbedo RF'), aerodynamic roughness ('ΔRoughness'), and the partitioning of net radiation into sensible and latent turbulent heat fluxes ('ΔBowen'). (a) Clear-cut site – Deciduous site; (b) Clear-cut – Coniferous site; (c) Deciduous – Coniferous forest, 6-year. annual means are displayed legends.

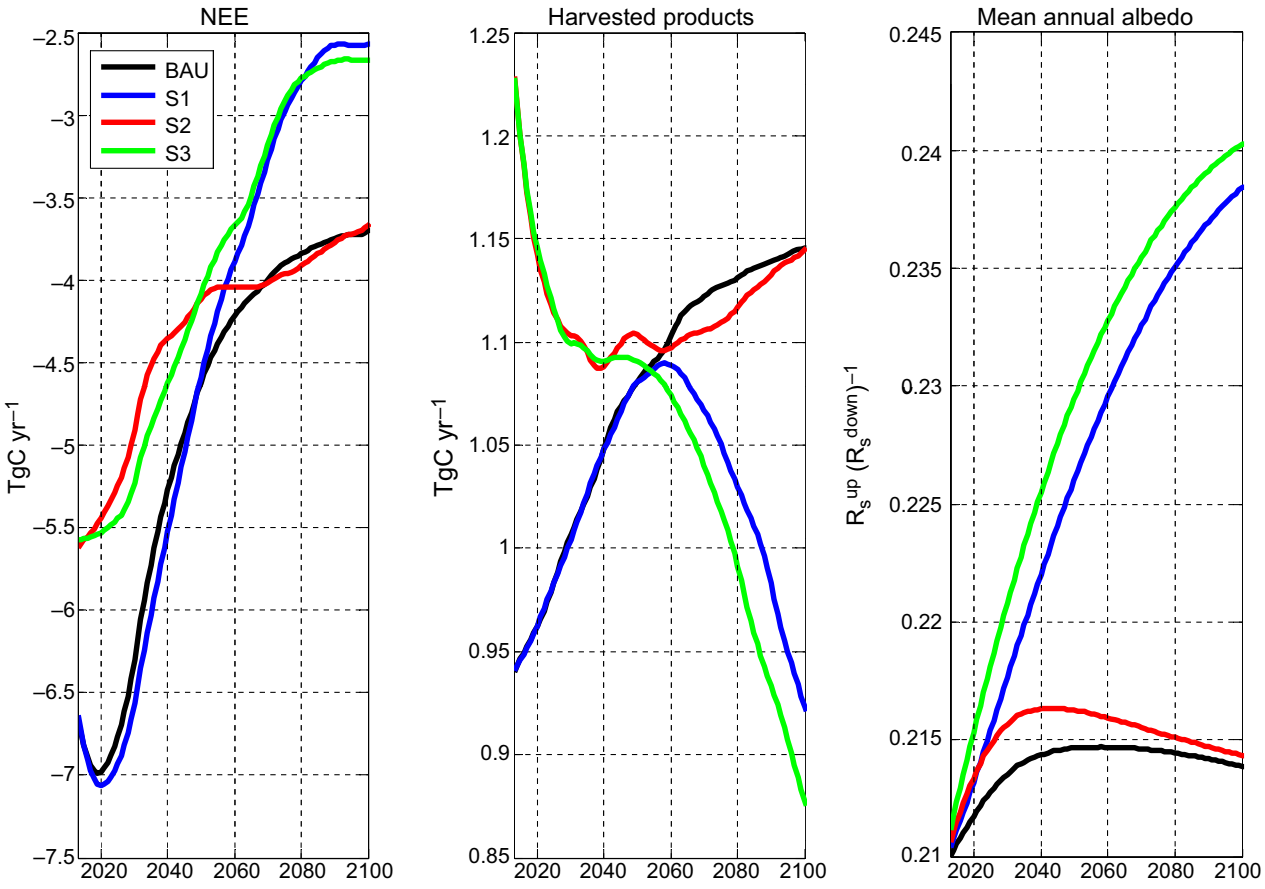

Fig. 3 Monte Carlo simulation mean (1,000 runs) NEE flux (left panel), Harvested Product flux (middle panel), and annual mean albedo trajectories (right panel) of the BAU and three alternative management scenarios.

S2 (red) relative to BAU due to a larger share of the coniferous area residing in clear-cut condition (young ages) with low snow masking.

When regional 21st century temperature forecasts connected to RCP4.5 and 8.5 are fed into the albedo model to approximate the magnitude of climate-albedo feedback, we find substantial reductions in the albedo of managed forest area in spring and autumn months (Fig. 4) – months particularly susceptible to strong snow-albedo feedback (Hall & Qu, 2006; Winton, 2006). For the BAU scenario, in relative terms the regional temperature change feedback on albedo in spring is equally pronounced in March as in April, where the albedo (blue curves) at 2100 is reduced by 12–26% in March and 16–24% in April under RCP4.5 and RCP8.5, respectively (see Fig. S6 for absolute values). In autumn, the albedo reduction at the end of the 21st century is more marked in November than October, where albedo is reduced up to 18 and 32% under RCP4.5 and 8.5, respectively. For the most extreme warming scenario (RCP8.5), when averaged over the year, the albedo in managed forests is reduced −0.011 (5%) at 2060 and −0.034 (16%) at 2100 (not shown). Following Betts (2000), applying Eqn (7) with an updated airborne fraction of 0.45 (Canadell *et al.*, 2007), we estimate the climate impact of this reduction – expressed in terms of an equivalent NEE C-flux – to be ca. 5.6 Tg C yr^{-1} at 2060 and ca. 28 Tg C yr^{-1} at 2100 – the latter estimate being approximately an eightfold increase in magnitude from the simulated NEE flux at 2100 for the BAU scenario.

Using global mean near surface temperature as a metric, the resulting direct climate impact from management-induced CO_2 concentration (from ΔNEE) and albedo changes (presented in Fig. 3) are plotted in Fig. 5, with the full range of climate-albedo feedback effects indicated in light blue, and the full range of carbon cycle-climate effects from decreasing CO_2 radiative efficiencies (see SI for details) indicated in light red.

Contributions from ΔNEE dominate the net temperature response when harvest intensities are increased and traditional silviculture methods go unaltered, as in S2 (Fig. 5, solid red line). However, for the two birch scenarios S1 and S3, cooling from albedo changes (Fig. 5, solid blue) play a significant role in offsetting carbon cycle impacts such that under S1 (left), a net

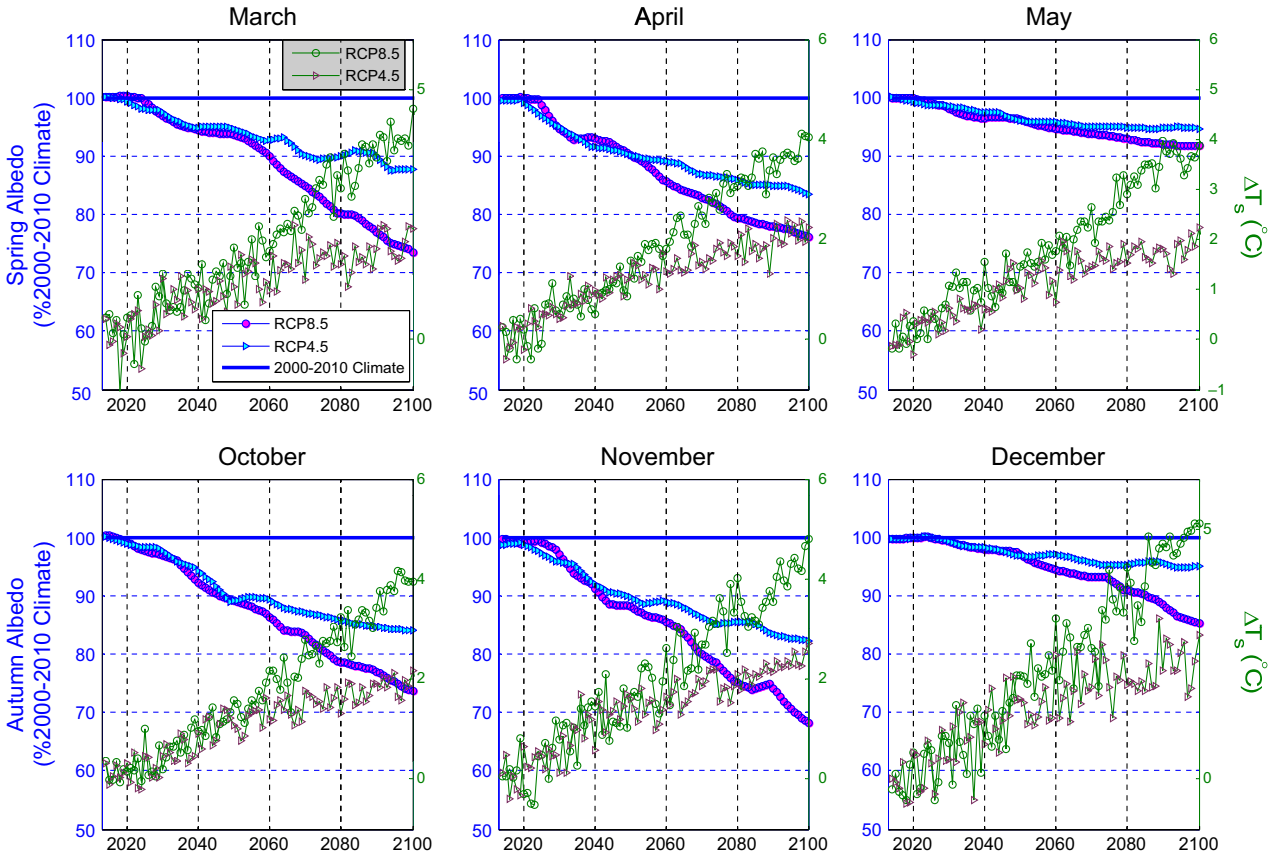

Fig. 4 Normalized Monte Carlo simulation mean (1,000 runs) spring and autumn albedo trajectories (lefthand *y*-axis, blue line colors) in the BAU scenario under projected regional climate warming (right-hand *y*-axis, green line colors).

cooling is realized over the entire 21st century, and under S3, for the latter four decades of the century. Increasing the harvest intensity (Fig. 3, middle) in the early decades under S3 relative to BAU diminishes the forest C-sink productivity more than increases in the share of deciduous stands enhance albedo, leading to slight net relative warming until 2060, with long-term net cooling thereafter (Fig. 5, black). In S3, the effect of CO_2's decreasing radiative efficiency in the atmosphere (Fig. 5, red dotted/dashed curves) from increasing background CO_2 concentrations approximately equals and offsets the magnitude of the regional warming feedback on albedo (Fig. 5, blue dotted/dashed curves) in the two RCP scenarios. Since ΔNEE switches sign about halfway through the 21st century in S1, the effect of a diminished CO_2 radiative efficiency under RCP scenarios is less pronounced.

Measured with the Global Temperature Potential (GTP) (Shine *et al.*, 2005; Forster *et al.*, 2007), Fig. 6 indicates the net warming potential of the three alternative management scenarios relative to BAU at any future point in the 21st century in terms of an equivalent CO_2 emission pulse today – plotted against the cumulative *HP* C-flux in each scenario. While the largest climate cooling benefits (negative GTP) are realized under S1 (triangle markers), these benefits comes at the expense of a reduced material supply relative to BAU (black markers, *x*-axis) in the latter decades of the 21st century (2070–2100), indicated in Fig. 6 (colorbar).

Figure 6 illustrates that, in general, the change in the accumulated quantity of harvested biomass across scenarios (*x*-axis) is smaller in relation to the difference in GTP – particularly for S1 and S2 – whose signs are in drastic opposition. At 2100, a management scenario resembling S2 yields an extra 3.75 Tg C of accumulated *HP* relative to BAU at a climate cost of over 170 Tg CO_2-eq. emitted today, while S3 yields a climate benefit equal to 158 Tg-CO_2-eq. of avoided emissions today at a cost of 4.5 Tg C less total *HP* by at 2100. Under S3, each additional cumulative Tg C *HP* relative to BAU results in approximately 12–15 additional Tg-CO_2-eq. of warming for the first five decades relative to 30–70 Tg-CO_2-eq. per additional Tg C in S2. Thanks to the albedo cooling benefits linked to the increased deciduous area, the sign of the modest near-term GTP penalties incurred in S3 switches such that a net global cooling (negative GTP) benefit is realized when one takes a longer term

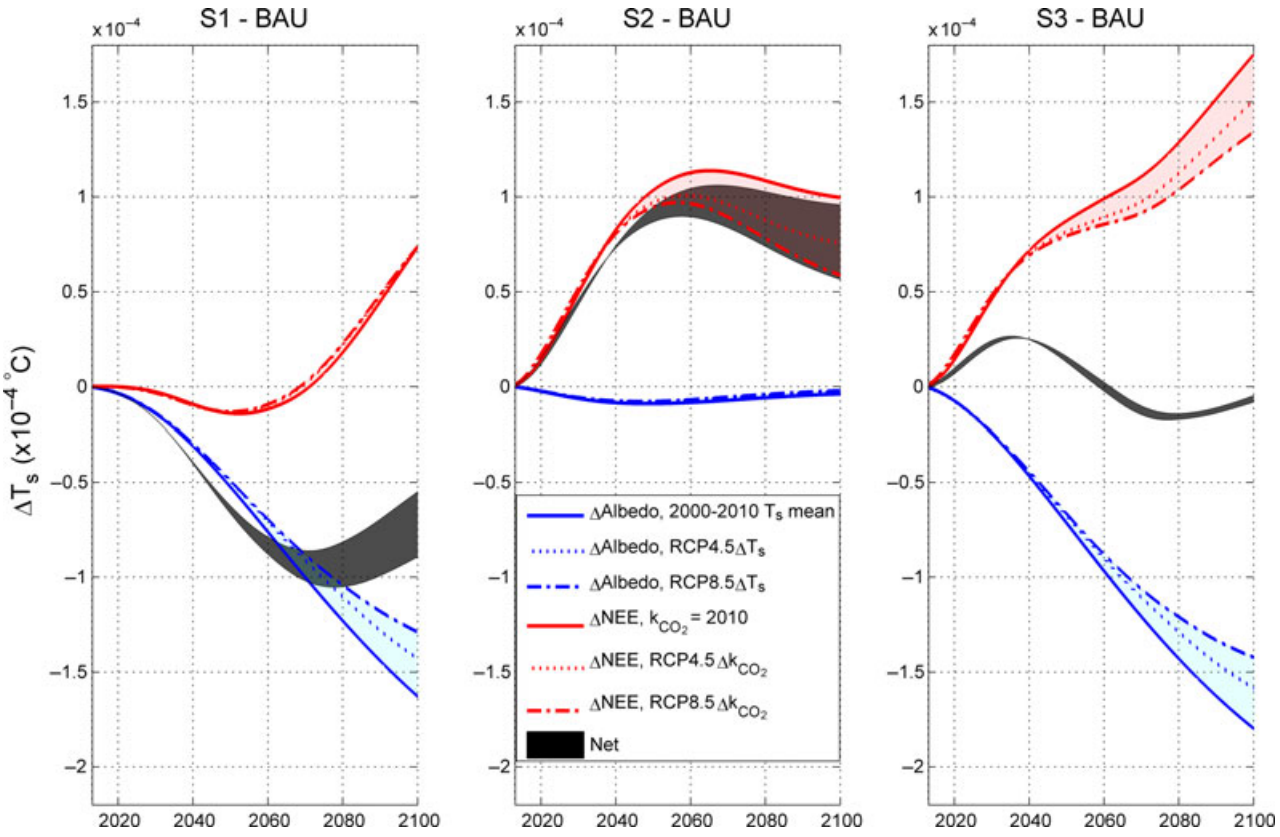

Fig. 5 Global mean surface temperature change due to changes in surface albedo (blue) and atmospheric CO_2 concentration changes resulting from changes in NEE (red) between the three alternative and the BAU forest management scenario. Black bands represent the range of net outcomes when temperature-albedo feedbacks and radiative efficiency changes under RCP4.5 and RCP8.5 scenarios are taken into consideration.

perspective. Fig. 6 illustrates the tough decisions policy makers will be faced with surrounding near- vs. long-term trade-offs in the material supply and global climate impact.

Discussion

Our results suggest that substantial climate protection benefits directly attributable to forest management can be realized by shifting to a regeneration strategy that favors more deciduous species. Due largely to its higher summer- and wintertime albedo, deciduous stands cooled both local and global near-surface temperatures relative to coniferous stands when averaged throughout the year (Fig. 2c). In summer, the external albedo forcing at the deciduous site combined with more efficient partitioning of R_n into latent heat outweighed the relative warming from a lowered surface roughness, resulting in net annual local cooling relative to the neighboring coniferous site, a finding in agreement with others (Baldocchi *et al.*, 2000; Chapin *et al.*, 2000; Blanken *et al.*, 2001; Liu *et al.*, 2005). In general, our results align with other observational evidence regarding the relative importance of albedo as the dominant direct biophysical mechanism influencing local climate by forests in boreal regions (Lee *et al.*, 2011). Over 6 years, T_s at a clear-cut site was found to be 0.25 °C cooler than at a nearby mature coniferous site due mostly to the external albedo forcing, although this estimate is less than values reported in Lee *et al.* (2011) for a coniferous site in the same latitude zone. This lower result is not unexpected, however, due to differences in vegetation cover and structural properties between the reference sites, where we have chosen an actual clear-cut site with tree retention and significant understory vegetation and Lee *et al.* (2011) 'open grassy fields'. Additionally, roughness and Bowen ratio warming at our clear-cut site could be underestimated due to the assertion that MOD16A2 overestimates LAI and FPAR at young disturbance sites in boreal regions (Serbin *et al.*, 2013). LAI and FPAR are key parameters in determining fractional vegetation coverage, roughness lengths, and evapotranspiration (see Supporting Information for additional detail).

Across the landscape, allowing more coniferous stands to be regenerated with birch (*Betula* spp.)

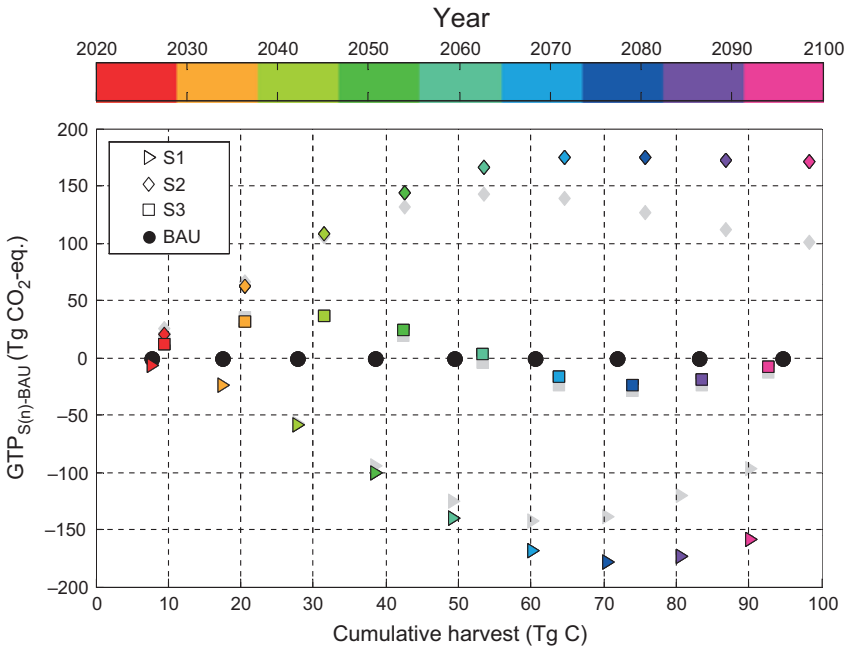

Fig. 6 The Global Temperature Potential of the three alternative forest management scenarios relative to the BAU scenario (*y*-axis) shown in relation to the cumulative Harvested Products C-flux (*x*-axis) of each scenario. The terrestrial C-cycle contribution to GTP impacts are calculated after subtracting C removed in lateral transfers (Harvested Products) from forests in each scenario, i.e. GTP equals the sum of changes in net ecosystem carbon balances (NECB) plus changes in albedo between any of the three alternative scenarios and BAU. GTPs with climate-albedo feedbacks and radiative efficiency changes linked to RCP8.5 are indicated in light gray.

considerably enhanced the overall albedo of the forest (Fig. 3) which led to substantial global climate cooling benefits throughout the 21st century (Scenario 1, Figs 5 and 6). Increasing regional harvest intensities simultaneously over BAU levels was found to offset the increased global warming from near-term reductions in the forest carbon sink, resulting in net global cooling over the longer term horizon (Scenario 3, Figs 5 and 6). These results indicate that boreal resource managers are faced with important trade-offs between long-term harvest volume preservation and climate impact across varying points in time depending on the management strategy pursued. Maintaining current silviculture regimes but increasing harvest intensities in the near term (Scenario 2) will allow sustained levels of material outtake from regional forests at the end of the 21st century – yet at a substantial warming penalty (Fig. 6). If climate protection is prioritized, however, maintaining current harvest intensities but increasing the share of deciduous stands in regional forests (Scenario 1) will maximize near-term climate cooling benefits – albeit at the expense of some reductions in the longer term material supply (Fig. 6). A compromise between the two differing strategies resembles that of S3, a scenario in which near-term harvests levels can be increased while still providing medium- to longer term climate cooling benefits. Although the long-term material supply is reduced, this reduction is less pronounced than in S1 and will not be incurred until the last decade. It should be reiterated that the reduction in the HP flux in S1 and S3 in the latter half of the 21st century (Fig. 3, middle) is not necessarily due to a stock reduction, but rather, due to the lower predicted harvest probability by the harvest model employed in the analysis (and thus less HP).

Medium- to long-term regional temperature-albedo feedback under RCP 4.5 and 8.5 reduced the global climate cooling benefits afforded by the enhanced forest albedo in management scenarios S1 and S3 (Fig. 5, light blue) relative to BAU. When jointly considering the reductions in the radiative efficiency of CO_2 in the atmosphere associated with the projected increases in atmospheric CO_2 concentration in RCP4.5 and 8.5, however, the global warming impact from a weakened forest carbon sink (Fig. 5, light red) relative to BAU was reduced. In S3, this reduction was found to be approximately equal in magnitude to the reduction in albedo change cooling benefits.

Monthly albedo analysis of the BAU scenario revealed that reductions in surface albedo from the projected regional temperature increases under global warming were most pronounced in late spring and autumn (Fig. 4) for both RCP scenarios – a time when the region is particularly sensitive to rapid snow-albedo feedbacks (Hall & Qu, 2006; Winton, 2006). Keeping the

focus on BAU, the implication of the reduced (annually averaged) forest albedo under RCP8.5 relative to a constant climate scenario is disturbing: net ecosystem exchange (productivity) would have to decrease (increase) eightfold by 2100 to counter the impact on global mean surface temperatures. Although the terrestrial C-cycle response to future regional warming was excluded from this study due to the large uncertainty in both the magnitude and even the sign of NEE for our region (Koca *et al*., 2006; Ahlström *et al*., 2012), these productivity increases are highly unlikely, as RCP8.5 multimodel mean outcomes from recent CMIP5 simulations indicate that forests in the latitude band 60–70°N are likely to become substantially weakened by the end of the century (Ahlström *et al*., 2012).

While we have attributed only those climate impacts induced by changes occurring within the forest to changes in forest management – additional impact linked to life-cycle emissions and to changes in the global supply and demand of timber products ought to be factored into any mitigation-oriented climate policy. Nevertheless, our study offers important general insights that may be extrapolated to other climatically similar boreal regions. Due to reduced snow masking in winter and spring combined with a higher canopy albedo in summer, management objectives targeting the replacement of coniferous stands with deciduous species serve to increase the overall albedo of the forested landscape which we demonstrate has both local and global climate cooling benefits, particularly over the near term. Our results lend support to the argument that a carbon-only focus in the design and implementation of forest management policy in boreal and other climatically similar regions can be counterproductive – and at best – suboptimal if forests are to be used as a tool to mitigate global warming.

Acknowledgements

We thank three anonymous reviewers for their constructive and valuable feedback. All MODIS Collection 5 subsetted land products were provided by Oak Ridge National Laboratory Distributed Active Archive Center (ORNL DAAC), Oak Ridge, Tennessee, USA, (http://daac.ornl.gov/MODIS/modis.html). This work was performed under the project 'Decision Support Models for Increased Harvest and Climate-motivated Forest Policies' funded by the Norwegian Research Council, grant number: 210464.

References

Ahlström A, Schurgers G, Arneth A, Smith B (2012) Robustness and uncertainty in terrestrial ecosystem carbon response to CMIP5 climate change projections. *Environmental Research Letters*, **7**, 044008.

Allen RG, Pereira LS, Raes D, Smith M (1998) *Crop evapotranspiration - Guidelines for computing crop water requirements - FAO irrigation and drainage paper 56*. FAO, Rome, Italy, UN.

Amiro BD, Orchansky AL, Barr AG *et al*. (2006) The effect of post-fire stand age on the boreal forest energy blance. *Agricultural and Forest Meteorology*, **140**, 41–50.

Anderson RG, Canadell JG, Randerson JT *et al*. (2010) Biophysical considerations in forestry for climate protection. *Frontiers in Ecology & Environment*, **9**, 174–182.

Anderson-Teixeira K, Snyder P, Twine T, Cuadra S, Costa M, Delucia E (2012) Climate-regulation services of natural and agricultural ecoregions of the Americas. *Nature Clim Change*, **2**, 177–181.

Angelstam PK (1998) Maintaining and restoring biodiversity in European boreal forests by developing natural disturbance regimes. *Journal of Vegetation Science*, **9**, 593–602.

Antón-Fernández C, Astrup R (2012) Empirical harvest models and their use in regional business-as-usual scenarios of timber supply and carbon stock development. *Scandinavian Journal of Forest Research*, **27**, 379–392.

Bala G, Caldeira K, Wickett M, Phillips TJ, Lobell DB, Delire C, Mirin A (2007) Combined climate and carbon-cycle effects of large-scale deforestation. *PNAS*, **104**, 6550–6555.

Baldocchi DD, Kelliher FM, Black A, Jarvis P (2000) Climate and vegetation controls on boreal zone energy exchange. *Global Change Biology*, **6**, 69–83.

Bathiany S, Claussen M, Brovkin V, Raddatz T, Gayler V (2010) Combined biogeophysical and biogeochemical effects of large-scale forest cover changes in the MPI earth system model. *Biogeosciences*, **7**, 1383–1399.

Beck PSA, Goetz SJ, Mack MC, Alexander HD, Randerson JT, Loranty MM (2011) The impacts and implications of an intensifying fire regime on Alaskan boreal forest composition and albedo. *Global Change Biology*, **17**, 2853–2866.

Bellouin N, Boucher O (2010) Climate response and efficacy of snow albedo forcings in the HadGEM2-AML climate model. Hadley Centre Technical Note, HCTN82, UK Met Office.

Betts RA (2000) Offset of the potential carbon sink from boreal forestation by decreases in surface albedo. *Nature*, **408**, 187–190.

Betts R (2007) Implications of land ecosystem-atmosphere interactions for strategies for climate change adaptation and mitigation. *Tellus B*, **59**, 602–615.

Betts AK, Ball JH (1997) Albedo over the boreal forest. *Journal of Geophysical Research*, **102**, 28901–28909.

Blanken PD, Black TA, Neumann HH, Den Hartog G, Yang PC, Nesic Z, Lee X (2001) The seasonal water and energy exchange above and within a boreal aspen forest. *Journal of Hydrology*, **245**, 118–136.

Bonan GB (2008) Forests and Climate Change: forcings, Feedbacks, and the Climate Benefits of Forests. *Science*, **320**, 1444–1449.

Bond-Lamberty B, Peckham SD, Gower ST, Ewers BE (2009) Effects of fire on regional evapotranspiration in the central Canadian boreal forest. *Global Change Biology*, **15**, 1242–1254.

Boucher O, Reddy MS (2008) Climate trade-off between black carbon and carbon dioxide emissions. *Energy Policy*, **36**, 193–200.

Bright RM, Kvalevåg MM (2013) Technical note: evaluating a simple parameterization of radiative shortwave forcing from surface albedo change. *Atmospheric Chemistry and Physics*, **13**, 11169–11174.

Bright RM, Strømman AH, Peters GP (2011) Radiative Forcing Impacts of Boreal Forest Biofuels: a Scenario Study for Norway in Light of Albedo. *Environmental Science & Technology*, **45**, 7570–7580.

Bright RM, Astrup R, Strømman AH (2013) Empirical models of monthly and annual albedo in managed boreal forests of interior Norway. *Climatic Change*, **120**, 183–196.

Burton PJ, Messier C, Adamowicz WL, Kuuluvainen T (2006) Sustainable management of Canada's boreal forests: progress and prospects1. *Ecoscience*, **13**, 234–248.

Canadell JG, Raupach MR (2008) Managing Forests for Climate Change Mitigation. *Science*, **320**, 1456–1457.

Canadell JG, Le Quéré C, Raupach MR *et al*. (2007) Contributions to accelerating atmospheric CO2 growth from economic activity, carbon intensity, and efficiency of natural sinks. *Proceedings of the National Academy of Sciences*, **104**, 18866–18870.

Chapin FS, Mcguire AD, Randerson J *et al*. (2000) Arctic and boreal ecosystems of western North America as components of the climate system. *Global Change Biology*, **6**, 211–223.

Chen HY, Popadiouk RV (2002) Dynamics of North American boreal mixedwoods. *Environmental Reviews*, **10**, 137–166.

Cherubini F, Bright RM, Strømman AH (2012) Site-specific global warming potentials of biogenic CO_2 for bioenergy: Contributions from carbon fluxes and albedo dynamics. *Environmental Research Letters*, **7**, 045902.

Cherubini F, Bright RM, Strømman AH (2013) Climate impacts of forest bioenergy: what, when, and how to measure? *Environmental Research Letters*, **8**, 014049. doi:014010.011088/011748-019326/014048/014041/014049.

Christensen M, Emborg J (1996) Biodiversity in natural versus managed forest in Denmark. *Forest Ecology and Management*, **85**, 47–51.

Ciais P, Schelhaas MJ, Zaehle S *et al*. (2008) Carbon accumulation in European forests. *Nature Geoscience*, **1**, 425–429.

Conway T, Tans PP (2012) Globally averaged marine surface annual mean data, Available at: www.esrl.noaa.gov/gmd/ccgg/trends/. NOAA/ESRL.

Davidson EA, Janssens IA (2006) Temperature sensitivity of soil carbon decomposition and feedbacks to climate change. *Nature*, **440**, 165–173.

Davin EL, De Noblet-Ducoudré N (2010) Climatic impact of global-scale deforestation: radiative versus nonradiative processes. *Journal of Climate*, **23**, 97–112.

De Wit HA, Palosuo T, Hylen G, Liski J (2006) A carbon budget of forest biomass and soils in southeast Norway calculated using a widely applicable method. *Forest Ecology and Management*, **225**, 15–26.

Dye DG, Tucker CJ (2003) Seasonality and trends of snow-cover, vegetation index, and temperature in northern Eurasia. *Geophysical Research Letters*, **30**, 1405.

Eugster W, Rouse WR, Pielke RA Sr *et al*. (2000) Land-atmosphere energy exchange in Arctic tundra and boreal forest: available data and feedbacks to climate. *Global Change Biology*, **6**, 84–115.

Forster P, Ramaswamy V, Artaxo P *et al*. (2007) Changes in atmospheric consituents and in radiative forcing. In: *Climate Change 2007: The Physical Science Basis. Contribution of Working Group I to the Fourth Assessment Report of the Intergovernmental Panel on Climate Change*. (eds Soloman S, Qin D, Manning M, Chen Z, Marquis M, Averyt KB, Tignor M, Miller HL) pp. 129–234 , Cambridge University Press, Cambridge, U. K. and New York, NY, USA.

Friedlingstein P, Cox P, Betts R *et al*. (2006) Climate–Carbon Cycle Feedback Analysis: results from the C4MIP Model Intercomparison. *Journal of Climate*, **19**, 3337–3353.

Fries C, Johansson O, Pettersson B, Simonsson P (1997) Silvicultural models to maintain and restore natural stand structures in Swedish boreal forests. *Forest Ecology and Management*, **94**, 89–103.

Gower ST, Krankina O, Olson RJ, Apps M, Linder S, Wang C (2001) Net Primary Production and Carbon Allocation Patterns of Boreal Forest Ecosystems. *Ecological Applications*, **11**, 1395–1411.

Granhus A, Fløistad IS (2010) Naturlig foryngelse etter markberedning på middels bonitet (G14) [Natural regeneration after scarification on medium site index (G14)]. Norwegian Forest and Landscape Institute, Ås, Norway Available at: http://www.skogoglandskap.no/filearchive/forskning_01_10_naturlig_foryngelse_etter_markberedning_middels_bonitet.pdf (accessed 16 April 2013).

Granhus A, Hylen G, Nilsen J-EØ (2012) Skogen i Norge. Statistikk over skogforhold og skogressurser i Norge registrert i perioden 2005–2009 [Statistics of forest conditions and forest resources in Norway registered in 2005–2009]. Ressursoversikt fra Skog og Landskap 03/12 [Resource overview from the Norwegian Forest and Landscape Institute report number 03/12] Available at: http://www.skogoglandskap.no/publikasjon/skogen_i_norge_statistikk_over_skogforhold_og_skogressurser_i_norge_registrert_i_perioden_2005_2009 (accessed 11 March 2013).

Hall A, Qu X (2006) Using the current seasonal cycle to constrain snow albedo feedback in future climate change. *Geophysical Research Letters*, **33**, L03502.

Hansen J, Sato M, Ruedy R *et al*. (2005) Efficacy of climate forcings. *Journal of Geophysical Research: Atmospheres*, **110**, D18104.

Hayes DJ, Turner DP, Stinson G *et al*. (2012) Reconciling estimates of the contemporary North American carbon balance among terrestrial biosphere models, atmospheric inversions, and a new approach for estimating net ecosystem exchange from inventory-based data. *Global Change Biology*, **18**, 1282–1299.

Holtsmark B (2012) Harvesting in boreal forests and the biofuel carbon debt. *Climatic Change*, **112**, 415–428.

Houspanossian J, Nosetto M, Jobbágy EG (2013) Radiation budget changes with dry forest clearing in temperate Argentina. *Global Change Biology*, **19**, 1211–1222.

Hudiburg TW, Law BE, Wirth C, Luyssaert S (2011) Regional carbon dioxide implications of forest bioenergy production. *Nature Clim Change*, **1**, 419–423.

Jackson RB, Randerson JT, Canadell JG *et al*. (2008) Protecting climate with forests. *Environmental Research Letters*, **3**, 044006 (044005 pp).

Joos F, Roth R, Fuglestvedt JS *et al*. (2013) Carbon dioxide and climate impulse response functions for the computation of greenhouse gas metrics: a multi-model analysis. *Atmospheric Chemistry and Physics*, **13**, 2793–2825.

Joshi M, Shine K, Ponater M, Stuber N, Sausen R, Li L (2003) A comparison of climate response to different radiative forcings in three general circulation models: towards an improved metric of climate change. *Climate Dynamics*, **20**, 843–854.

Juang J-Y, Katul G, Siqueira M, Stoy P, Novick K (2007) Separating the effects of albedo from eco-physiological changes on surface temperature along a successional chronosequence in the southeastern United States. *Geophysical Research Letters*, **34**, L21408.

KNMI (2013) *CMIP5 Scenario Runs - Surface Variables*. Accessed 15.3.2013 at: http://climexp.knmi.nl/selectfield_cmip5.cgi?id=rtisdale@snet.net. Royal Meterological Insitute of The Netherlands (KNMI) Climate Explorer.

Knyazikhin Y, Glassy J, Privette JL *et al*. (1999) MODIS Leaf Area Index (LAI) and Fraction of Photosynthetically Active Radiation Absorbed by Vegetation (FPAR) Product (MOD15): Algorithm Theoretical Basis Document Version 4.0, http://eospso.gsfc.nasa.gov/atbd/modistables.html.

Koca D, Smith B, Sykes MT (2006) Modelling regional climate change effects on potential natural ecosystem in Sweden. *Climatic Change*, **78**, 381–406.

Kustas WP, Daughtry CST (1990) Estimation of the soil heat flux/net radiation ratio from spectral data. *Agricultural and Forest Meteorology*, **49**, 205–223.

Kuuluvainen T (2009) Forest Management and Biodiversity Conservation Based on Natural Ecosystem Dynamics in Northern Europe: the Complexity Challenge. *AMBIO: A Journal of the Human Environment*, **38**, 309–315.

Lamers P, Junginger M, Dymond CC, Faaij A (2013) Damaged forests provide an opportunity to mitigate climate change. *Global Change Biology Bioenergy*, doi: 10.1111/gcbb.12055. [Early view].

Lapenis A, Shvidenko A, Shepaschenko D, Nilsson S, Aiyyer A (2005) Acclimation of Russian forests to recent changes in climate. *Global Change Biology*, **11**, 2090–2102.

Lee X, Goulden ML, Hollinger DY *et al*. (2011) Observed increase in local cooling effect of deforestation at higher latitudes. *Nature*, **479**, 384–387.

Lenton TM, Vaughan NE (2009) The radiative forcing potential of different climate geoengineering options. *Atmospheric Chemistry and Physics Discussions*, **9**, 5539–5561.

Lieffers VJ, Beck JA Jr (1994) A semi-natural approach to mixedwood management in the prairie provinces. *The Forestry Chronicle*, **70**, 260–264.

Lindroth A, Grelle A, Morén A-S (1998) Long-term measurements of boreal forest carbon balance reveal large temperature sensitivity. *Global Change Biology*, **4**, 443–450.

Liski J, Palosuo T, Peltoniemi M, Sievänen R (2005) Carbon and decomposition model Yasso for forest soils. *Ecological Modelling*, **189**, 168–182.

Liu H, Randerson JT, Lindfors J, Chapin FS (2005) Changes in the surface energy budget after fire in boreal ecosystems of interior Alaska: an annual perspective. *Journal of Geophysical Research: Atmospheres*, **110**, D13101.

Liu S, Lu L, Mao D, Jia L (2007) Evaluating parameterizations of aerodynamic resistance to heat transfer using field measurements. *Hydrology and Earth System Sciences*, **11**, 769–783.

Lohila A, Minkkinen K, Laine J *et al*. (2010) Forestation of boreal peatlands: impacts of changing albedo and greenhouse gas fluxes on radiative forcing. *Journal of Geophysical Research: Biogeosciences*, **115**, 1–15.

Los SO, Pollack NH, Parris MT *et al*. (2000) A global 9-yr Biophysical Land Surface Dataset from NOAA AVHRR Data. *Journal of Hydrometeorology*, **1**, 183–199.

Lukeš P, Stenberg P, Rautiainen M (2013) Relationship between forest density and albedo in the boreal zone. *Ecological Modelling*, **261–262**, 74–79.

Macdonald GB (1995) The case for boreal mixedwood management: an Ontario perspective. *The Forestry Chronicle*, **71**, 725–734.

Mackey B, Prentice IC, Steffen W, House JI, Lindenmayer D, Keith H, Berry S (2013) Untangling the confusion around land carbon science and climate change mitigation policy. *Nature Clim Change*, **3**, 552–557.

Mahmood R, Pielke RA, Hubbard KG *et al*. (2013) Land cover changes and their biogeophysical effects on climate. *International Journal of Climatology*. doi:10.1002/joc.3736 [Early view].

Mann ME, Park J (1996) Greenhouse warming and changes in the seasonal cycle of temperature: model versus observations. *Geophysical Research Letters*, **23**, 1111–1114.

Marklund LG (1988) *Biomassafunktioner for tall, gran och björk i Sverige [Biomass functions for pine, spruce, and birch in Sweden]* (Report No. 45). Department of Forestry, Swedish University of Agricultural Sciences, Umeå, Sweden. (In Swedish with English summar).

Marland G, Pielke RA, Apps M *et al*. (2003) The climatic impacts of land surface change and carbon management, and the implications for climate-change mitigation policy. *Climate Policy*, **3**, 149–157.

Monteith JL, Unsworth MH (eds.) (2008) *Principles of environmental physics (3rd edn)*. Elsevier Academic Press, London. ISBN 978-0-12-505103-3.

Mu Q, Zhao M, Running SW (2011) Improvements to a MODIS global terrestrial evapotranspiration algorithm. *Remote Sensing of Environment*, **115**, 1781–1800.

Myhre G, Highwood EJ, Shine KP, Stordal F (1998) New estimtes of raditive forcing due to well mixed greenhouse gases. *Geophysical Research Letters*, **25**, 2715–2718.

Nakai T, Sumida A, Daikoku K *et al*. (2008) Parameterisation of aerodynamic roughness over boreal, cool- and warm-temperate forests. *Agricultural and Forest Meteorology*, **14**, 1916–1925.

NASA (2013) *Prediction of Worldwide Energy Resource (POWER)*. NASA Langley Research Center. Accessed May 3, 2013 at: http://power.larc.nasa.gov/common/php/POWER_AboutPOWER.php.

Norwegian Meteorological Institute (2013) *eKlima - Monthly Historical Meteorology*. Norwegian Meteorological Institute. Accessed Jan 31, 2013 at: http://sharki.oslo.dnmi.no/portal/page?_pageid=73,39035,73_39049&_dad=portal&_schema=PORTAL.

Norwegian Ministry of Food and Agriculture (2009) *St. meld. nr. 39: Klimautfordringene - landbruket en del av løsningen [Climate change - the land use part of the solution]*. Norwegian Ministry of Food and Agriculture, Oslo.

O'halloran TL, Law BE, Goulden ML *et al*. (2012) Radiative forcing of natural forest disturbances. *Global Change Biology*, **18**, 555–565.

Pan Y, Birdsey RA, Fang J *et al*. (2011) A large and persistent carbon sink in the world's forests. *Science*, **333**, 988–993. doi:10.1126/science.1201609.

Peel MC, Finlayson BL, Mcmahon TA (2007) Updated world map of the Köppen-Geiger climate classification. *Hydrology and Earth System Sciences*, **11**, 1633–1644.

Pielke RA Sr, Pitman A, Niyogi D *et al*. (2011) Land use/land cover changes and climate: modeling analysis and observational evidence. *WIREs Climate Change*, **2**, 828–850.

Pongratz J, Reick CH, Raddatz T, Claussen M (2010) Biogeophysical versus biogeochemical climate response to historical anthropogenic land cover change. *Geophysical Research Letters*, **37**, L08702.

Pongratz J, Reick CH, Raddatz T, Caldeira K, Claussen M (2011) Past land use decisions have increased mitigation potential of reforestation. *Geophysical Research Letters*, **38**, L15701.

Randerson JT, Liu H, Flanner MG *et al*. (2006) The Impact of Boreal Forest Fire on Climate Warming. *Science*, **314**, 1130–1132.

Rautiainen A, Wernick I, Waggoner PE, Ausubel JH, Kauppi PE (2011) A National and International Analysis of Changing Forest Density. *PLoS ONE*, **6**, e19577. doi:19510.11371/journal.pone.0019577.

Riahi K, Rao S, Krey V *et al*. (2011) RCP 8.5—A scenario of comparatively high greenhouse gas emissions. *Climatic Change*, **109**, 33–57.

Rocha AV, Shaver GR (2011) Postfire energy exchange in arctic tundra: the importance and climatic implications of burn severity. *Global Change Biology*, **17**, 2831–2841.

Rotenberg E, Yakir D (2010) Contribution of semi-arid forests to the climate system. *Science*, **327**, 451–454.

Schaaf CB, Gao F, Strahler AH *et al*. (2002) First operational BRDF, albedo nadir reflectance products from MODIS. *Remote Sensing of Environment*, **83**, 135–148.

Serbin SP, Ahl DE, Gower ST (2013) Spatial and temporal validation of the MODIS LAI and FPAR products across a boreal forest wildfire chronosequence. *Remote Sensing of Environment*, **133**, 71–84.

Shine KP, Fuglestvedt JS, Hailemariam K, Stuber N (2005) Alternatives to the global warming potential for comparing climate impacts of emissions of greenhouse gases. *Climatic Change*, **68**, 281–302.

Sistla SA, Moore JC, Simpson RT, Gough L, Shaver GR, Schimel JP (2013) Long-term warming restructures Arctic tundra without changing net soil carbon storage. *Nature*, doi:10.1038/nature12129 [Advance online publication].

Sitch S, Huntingford C, Gedney N *et al*. (2008) Evaluation of the terrestrial carbon cycle, future plant geography and climate-carbon cycle feedbacks using five Dynamic Global Vegetation Models (DGVMs). *Global Change Biology*, **14**, 2015–2039.

Steyaert LT, Knox RG (2008) Reconstructed historical land cover and biophysical parameters for studies of land-atmosphere interactions within the eastern United States. *Journal of Geophysical Research*, **113**, D02101.

Stocks BJ, Fosberg MA, Lynham TJ *et al*. (1998) Climate Change and Forest Fire Potential in Russian and Canadian Boreal Forests. *Climatic Change*, **38**, 1–13.

Swann AL, Fung IY, Levis S, Bonan GB, Doney SC (2010) Changes in Arctic vegetation amplify high-latitude warming through the greenhouse effect. *PNAS*, **107**, 1295–1300.

Swann ALS, Fung I, Chiang JCH (2011) Mid-latitude afforestation shifts general circulation and tropical precipitation. *PNAS*, **109**, 712–716.

Thompson MP, Adams D, Sessions J (2009) Radiative forcing and the optimal rotation age. *Ecological Economics*, **68**, 2713–2720.

Thomson A, Calvin K, Smith S *et al*. (2011) RCP4.5: a pathway for stabilization of radiative forcing by 2100. *Climatic Change*, **109**, 77–94.

Tomter SM, Hylen G, Nilsen J-EØ (2010) Development of Norway's National Forest Inventory. In: *National Forest Inventories - Pathways for Common Reporting*. (eds Tomppo E, Gschwantner T, Lawrence M, Mcroberts RE) pp. 411–424. Springer, Heidelberg.

Van Cleve K, Viereck LA, Dyrness CT (1996) State Factor Control of Soils and Forest Succession along the Tanana River in Interior Alaska, U.S.A. *Arctic and Alpine Research*, **28**, 388–400.

Von Randow C, Manzi AO, Kruijt B *et al*. (2004) Comparative measurements and seasonal variations in energy and carbon exchange over forest and pasture in South West Amazonia. *Theoretical and Applied Climatology*, **78**, 5–26.

Wan Z (1999) *MODIS Land-surface temperature algorithm theoretical basic document (LST ATBD) version 3.3*. Institute for Computational Earth System Science, University of California, Santa Barbara.

Wan Z, Li Z-L (2008) Radiance-based validation of the V5 MODIS land-surface temperature product. *International Journal of Remote Sensing*, **29**, 5373–5395.

Wang K, Dickinson RE (2012) A review of global terrestrial evapotranspiration: observation, modeling, climatology, and climatic variability. *Review of Geophysics*, **50**, RG2005.

West PC, Narisma GT, Barford CC, Kucharik CJ, Foley JA (2011) An alternative approach for quantifying climate regulations by ecosystems. *Frontiers in Ecology & Environment*, **9**, 126–133.

Winton M (2006) Surface Albedo Feedback Estimates for the AR4 Climate Models. *Journal of Climate*, **19**, 359–365.

Xu L, Myneni RB, Chapin Iii FS *et al*. (2013) Temperature and vegetation seasonality diminishment over northern lands. *Nature Clim Change*, **3**, 581–586.

Supporting Information

Additional Supporting Information may be found in the online version of this article:

Data S1. Relative contributions to local climate change from changes to surface intrinsic biophysical mechanisms.
Data S2. Uncertainty.
Data S3. Modeling Adjustments: RCP Scenarios.
Data S4. Alternative Figures: Results.
Table S1. Overview of meteorological and remote sensing variables employed in the stand-level/local impact analysis.
Figure S1. Six-year mean 8-day MODIS ET, Black-sky Albedo, LAI, and FPAR observations at each stand in our local-scale analysis, shown with standard deviation as indicator of interannual variability. Biophysical variables are grouped by color and row, and sites are grouped by column. Data are for a single MODIS pixel of ca. 1 km^2. 6-year annual means and standard deviations are shown in legends.
Figure S2. Full 6-year time series of key radiative, aerodynamic, and physiological parameters applied in the stand-scale local climate impact analysis. Top: Roughness lengths for momentum (left) and aerodynamic resistances to heat and momentum transfer (right); Middle: Black-sky albedo at local solar noon (left) and Bowen ratios (right); Bottom: Leaf Area Index (left) and Fractional Vegetation Coverage (right).
Figure S3. Monte Carlo simulation mean (1000 replications) NEE flux, HP flux, and surface albedo for each scenario shown with one standard deviation.
Figure S4. Radiative efficiency per kg CO_2 emitted to the atmosphere for the two emission scenarios linked to representative concentration pathways (RCPs) 4.5 and 8.5 compared to the 2010 concentration of 389 ppm.
Figure S5. Full 6-year time series contributions to daily local surface temperature across three managed sites due to differences in surface albedo ('ΔAlbedo RF'), aerodynamic roughness ('ΔRoughness'), and the partitioning of net radiation into sensible and latent turbulent heat fluxes ('ΔBowen'). (A) Clear-cut site – Deciduous site; (B) Clear-cut – Coniferous site; (C) Deciduous – Coniferous forest.
Figure S6. Simulation means of absolute spring and autumn albedo trajectories (lefthand *y*-axis, blue line colors) in the BAU scenario under projected regional climate warming (right-hand *y*-axis, green line colors).